

Accessing baryon-antibaryon generalized distribution amplitudes in $e^\pm\gamma \rightarrow e^\pm B\bar{B}$

Jing Han,¹ Bernard Pire,² and Qin-Tao Song^{1,*}

¹*School of Physics, Zhengzhou University, Zhengzhou, Henan 450001, China*

²*CPHT, CNRS, École polytechnique, Institut Polytechnique de Paris, 91128 Palaiseau, France*

(Dated: November 11, 2025)

$\gamma^*\gamma \rightarrow B\bar{B}$ is the golden process to access chiral-even di-baryon generalized distribution amplitudes (GDAs) as deeply virtual Compton scattering has proven to be for the generalized parton distributions. In the framework of collinear QCD factorization where the leading twist amplitude is the convolution of GDAs and a perturbatively calculable coefficient function, we study the scattering amplitude for the baryonic channels where B is a spin 1/2 baryon such as the nucleon or hyperon Λ, Σ . Taking into account the interfering QED amplitude, we calculate the cross section of the $e^\pm\gamma \rightarrow e^\pm B\bar{B}$ process that can be experimentally studied in e^-e^+ as well as in electron-ion facilities. We explore both the final state polarization summed case and the polarization dependent effects. Numerical estimates are presented for $e^-\gamma \rightarrow e^-p\bar{p}$, using motivated models for GDAs. Our results show that a first extraction of baryon-antibaryon GDAs from experimental measurements is feasible at Belle II.

I. INTRODUCTION

Generalized distribution amplitudes (GDAs) [1–3] and the closely related generalized parton distributions (GPDs) [1, 4, 5] are hadronic matrix elements of light-cone bilocal operators that can be used for a hadron tomography [6–9]. Moreover, GDAs and GPDs offer an indirect access to the gravitational form factors (GFFs), which in turn enable us to address the longstanding puzzle of nucleon spin decomposition [4, 10–12] and to explore the mechanical properties of the hadron [13–26]. GDAs are the s - t crossed quantities of the hadronic GPDs, and both of them can be expressed in terms of the double distributions (DDs) [1, 5]. The DDs are often used to construct the GPD model for the extraction of GPDs from experimental measurements. Thus, the study of GDAs can provide us complementary information on GPDs, and vice versa. The second moments of GDAs give access to the timelike GFFs, from which the spacelike GFFs can be derived via dispersion relations.

As most hadrons are not stable, their GPDs are difficult to probe experimentally. In contrast, the hadronic GDAs can be studied through hadron pair production, which enables measurements for both stable and unstable hadrons. In the reactions $\gamma^*\gamma \rightarrow h\bar{h}$ and $\gamma^* \rightarrow h\bar{h}\gamma$, the momentum square of the virtual photon is chosen large enough to satisfy the QCD collinear factorization criteria. The amplitudes of these two-photon reactions can then be expressed in terms of the chiral-even hadronic GDAs, which describe the amplitudes for $q\bar{q} \rightarrow h\bar{h}$ [2, 27–36]. In addition, the authors of Ref. [37] recently proposed that chiral-odd hadronic GDAs can be extracted from the production of two meson pairs in e^+e^- annihilation. In 2016, the Belle Collaboration reported the first measurement of the cross section for $\gamma^*\gamma \rightarrow \pi^0\pi^0$ [38], from which the quark GDAs and GFFs of the pion were extracted [29]. With data taking recently underway at Belle II at much higher luminosity, measurements of $\gamma^*\gamma \rightarrow \pi^0\pi^0$ with unprecedented precision are expected in the near future.

For the production of a baryon-antibaryon pair, the amplitude of $\gamma^* \rightarrow B\bar{B}\gamma$ is expressed in terms of the baryon-antibaryon GDAs, where the virtual photon can come from e^+e^- annihilation, namely, $e^+e^- \rightarrow \gamma^* \rightarrow B\bar{B}\gamma$, and it is accessible at BESIII and the proposed Super Tau-Charm Facility (STCF) [39]. However, the initial state radiation process also contributes to $e^+e^- \rightarrow B\bar{B}\gamma$, and it is described by the timelike electromagnetic form factors (EM FFs) of the baryon [36]. Since extensive measurements of the timelike EM FFs of the baryon octet are already available [40–56], the baryon-antibaryon GDAs can be extracted from the future measurements of $e^+e^- \rightarrow B\bar{B}\gamma$. In this work, we study the baryon-antibaryon GDAs in the reaction $e^\pm\gamma \rightarrow e^\pm B\bar{B}$, which can be measured at Belle II, the proposed STCF, and electron-ion colliders [57] through ultraperipheral collisions. We also provide the polarization-dependent cross section for the final baryon or antibaryon, since the baryon spin vectors can be determined from their subsequent decays, such as $\Lambda \rightarrow N\pi$ and $\Sigma \rightarrow N\pi$, where N denotes a nucleon. The polarization-dependent cross section enables the definition of additional spin observables, from which further information on the GDAs can be extracted.

This paper is organized as follows. In Sec. II, we introduce the center-of-mass frame of the baryon-antibaryon pair in the process $e^\pm\gamma \rightarrow e^\pm B\bar{B}$ and define the twist-2 baryon-antibaryon GDAs as well as the baryon EM FFs. In

*songqintao@zzu.edu.cn

Sec. III, the hadron tensor of $\gamma^* \gamma \rightarrow B \bar{B}$ is expressed in terms of the timelike Compton FFs, and we then derive the corresponding cross sections, including the polarization of the final-state baryon. Numerical estimates for the cross sections, based on models of the baryon EM FFs and GDAs, are presented in Sec. IV. Finally, our main results are summarized in Sec. V.

II. GENERALIZED DISTRIBUTION AMPLITUDES IN $e^\pm \gamma \rightarrow e^\pm B \bar{B}$

We consider the production of a baryon-antibaryon pair in the following exclusive process,

$$e^\pm(k_1)\gamma(q_2) \rightarrow e^\pm(k_2)B(p_1, S_1)\bar{B}(p_2, S_2), \quad (1)$$

where the momenta are indicated in parentheses. We denote the spin vectors of the baryon and antibaryon as S_1 and S_2 , respectively, and these spin vectors can be determined from the subsequent decays of hyperons. To describe this process, it is convenient to define the following variables,

$$s = (k_1 + q_2)^2, \quad (k_1 - k_2)^2 = (q_1)^2 = -Q^2, \quad \hat{s} = P^2 = (p_1 + p_2)^2, \quad (p_1)^2 = (p_2)^2 = m^2, \quad (2)$$

where m is the baryon mass. We choose two lightcone vectors n and \tilde{n} , with $n \cdot \tilde{n} = 1$, which are built from the photon momenta q_1 and q_2 , as:

$$n = \frac{\sqrt{2}Q}{Q^2 + \hat{s}}q_2, \quad \tilde{n} = \frac{\sqrt{2}}{Q} \left(q_1 + \frac{Q^2}{Q^2 + \hat{s}}q_2 \right). \quad (3)$$

Then, the lightcone components $v^+ = v \cdot n$ and $v^- = v \cdot \tilde{n}$ are defined for a Lorentz vector v .

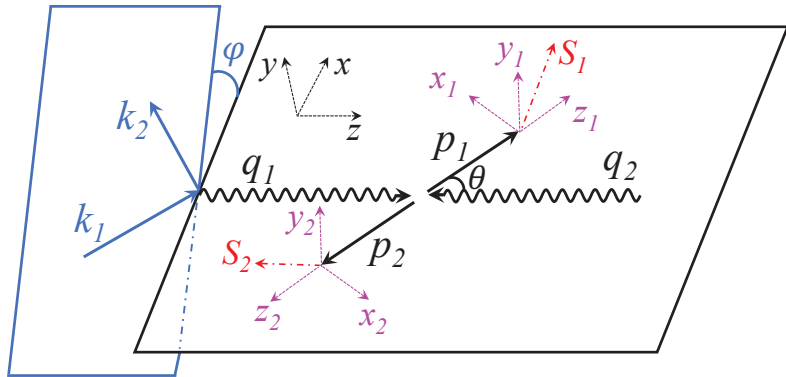


FIG. 1: The center-of-mass frame of the baryon-antibaryon pair for the process $e^\pm \gamma \rightarrow e^\pm B \bar{B}$.

The final cross sections will be presented in the center-of-mass frame of the baryon-antibaryon pair, as described by Fig. 1. We choose a coordinate system with the z axis along the momentum q_1 , and the baryon momenta p_1 and p_2 lie in the x - z plane. The polar angle of p_1 is denoted as θ , and φ is the azimuthal angle between the lepton plane and the hadron plane. These angles can be expressed in terms of Lorentz invariants,

$$\cos \theta = \frac{q_1 \cdot (p_2 - p_1)}{\beta_0 (q_1 \cdot q_2)},$$

$$\sin \varphi = \frac{4\epsilon_{\alpha\beta\gamma\delta} p_1^\alpha p_2^\beta k_1^\gamma q_1^\delta}{\beta_0 \sin \theta \sqrt{s} Q^2 \hat{s} (s - \hat{s} - Q^2)},$$

where the convention $\epsilon^{0123} = 1$ is used, and β_0 is the baryon velocity,

$$\beta_0 = \sqrt{1 - \frac{4m^2}{\hat{s}}}. \quad (4)$$

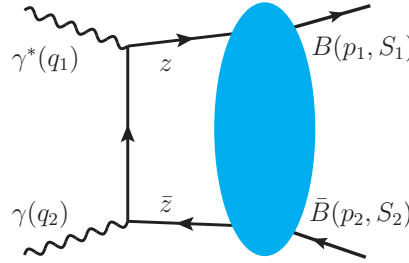


FIG. 2: The Feynman diagram for the QCD subprocess (a) $\gamma^* \gamma \rightarrow B \bar{B}$; the crossed diagram is obtained by interchanging the photon-quark vertices.

Note that the spin vectors S_1 and S_2 are defined within their own rest frames, namely $x_1 y_1 z_1$ and $x_2 y_2 z_2$ in Fig. 1. These vectors are given by

$$S_1^\mu = (0, S_1^x, S_1^y, S_1^z), \\ S_2^\mu = (0, S_2^x, S_2^y, S_2^z).$$

In $e^\pm \gamma \rightarrow e^\pm B \bar{B}$, the C -even baryon-antibaryon pairs can be produced in subprocess (a) where the real photon fuses with the virtual photon emitted by the lepton. The amplitude of this subprocess can be expressed in terms of the baryon GDAs using the QCD collinear factorization valid in the generalized Bjorken regime ($Q^2 \gg \hat{s}, \Lambda_{\text{QCD}}^2$) as illustrated by Fig. 2. The baryon GDAs are QCD nonperturbative quantities that describe the amplitude for the process $q\bar{q} \rightarrow B \bar{B}$. At leading-twist level, the amplitudes will be investigated using the twist-2 chiral-even GDAs for a baryon-antibaryon pair, which are defined as [58]

$$P^+ \int \frac{dx^-}{2\pi} e^{izP^+x^-} \langle \bar{B}(p_2)B(p_1) | \bar{q}(-x^-) \gamma^+ q(0) | 0 \rangle = \Phi_V^q(z, \zeta_0, \hat{s}) \bar{u}(p_1) \gamma^+ v(p_2) + \Phi_S^q(z, \zeta_0, \hat{s}) \frac{P^+}{2m} \bar{u}(p_1) v(p_2), \\ P^+ \int \frac{dx^-}{2\pi} e^{izP^+x^-} \langle \bar{B}(p_2)B(p_1) | \bar{q}(-x^-) \gamma^+ \gamma_5 q(0) | 0 \rangle = \Phi_A^q(z, \zeta_0, \hat{s}) \bar{u}(p_1) \gamma^+ \gamma_5 v(p_2) + \Phi_P^q(z, \zeta_0, \hat{s}) \frac{P^+}{2m} \bar{u}(p_1) \gamma_5 v(p_2), \quad (5)$$

where the lightcone gauge is used, and we omit to write the factorization scale dependence of the GDAs. In Eq. (5), z is the momentum fraction carried by the quark, and the skewness parameter ζ_0 is given by

$$\zeta_0 = \frac{\Delta \cdot n}{P \cdot n} \quad (6)$$

with $\Delta = p_2 - p_1$. This parameter is related to the baryon polar angle by $\zeta_0 = -\beta_0 \cos \theta$.

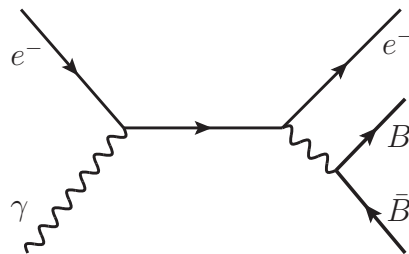


FIG. 3: The Feynman diagram for the bremsstrahlung subprocess (b) where the photon-baryon-antibaryon coupling is described by the timelike baryon EM FFs, the crossed diagram is obtained by interchanging the photon-lepton vertices.

The C -odd baryon-antibaryon pairs may originate from a virtual photon emitted by the lepton, which is denoted as subprocess (b) in Fig. 3. The amplitude of this subprocess can be written as the timelike baryon EM FFs,

$$\langle \bar{B}(p_2)B(p_1) | \bar{q}(0) \gamma^\mu q(0) | 0 \rangle = F_V^q(\hat{s}) \bar{u}(p_1) \gamma^\mu v(p_2) + F_S^q(\hat{s}) \frac{\Delta^\mu}{2m} \bar{u}(p_1) v(p_2), \quad (7)$$

and these FFs are also related to the first moments of baryon GDAs [58]. In the literature, the electric and magnetic

FFs G_E and G_M are commonly used, and they can be obtained from a linear combination of $F_V^q(\hat{s})$ and $F_S^q(\hat{s})$,

$$\begin{aligned} G_E(\hat{s}) &= \sum_q e_q [F_V^q(\hat{s}) + (\tau - 1)F_S^q(\hat{s})], \\ G_M(\hat{s}) &= \sum_q e_q F_V^q(\hat{s}), \end{aligned} \quad (8)$$

with $\tau = \hat{s}/(4m^2)$.

III. SCATTERING AMPLITUDES AND CROSS SECTIONS

A. Hadron tensor

In subprocess (a), C -even baryon-antibaryon pairs are produced, and the corresponding helicity amplitude can be written as

$$A_{\lambda_1 \lambda_2} = \epsilon_1^\mu(\lambda_1) T_{\mu\nu} \epsilon_2^\nu(\lambda_2), \quad (9)$$

where λ_1 and λ_2 denote the helicities of the virtual and real photons, respectively. The hadron tensor $T_{\mu\nu}$ is defined by the matrix element of the time-ordered product of two EM currents,

$$T_{\mu\nu} = i \int d^4x e^{-iq_1 \cdot x} \langle \bar{B}(p_2) B(p_1) | T\{j_\mu^{\text{em}}(x) j_\nu^{\text{em}}(0)\} | 0 \rangle. \quad (10)$$

At leading twist, the hadron tensor is expressed in terms of four timelike Compton FFs \mathcal{F}_i ,

$$T^{\mu\nu} = \frac{-\sqrt{2}}{Q} \left\{ g_T^{\mu\nu} \left[\zeta_0 \mathcal{F}_V \bar{u}(p_1) \gamma^+ v(p_2) + \mathcal{F}_S \frac{P^+}{2m} \bar{u}(p_1) v(p_2) \right] - i \epsilon_T^{\mu\nu} \left[\mathcal{F}_A \bar{u}(p_1) \gamma^+ \gamma^5 v(p_2) + \mathcal{F}_P \frac{P^+}{2m} \bar{u}(p_1) \gamma^5 v(p_2) \right] \right\}, \quad (11)$$

and these FFs are given at leading order in α_s by

$$\begin{aligned} \zeta_0 \mathcal{F}_V &= \sum_q \frac{e_q^2}{2} \int_0^1 dz \frac{2z-1}{z\bar{z}} \Phi_V^q(z, \zeta_0, \hat{s}), \\ \mathcal{F}_S &= \sum_q \frac{e_q^2}{2} \int_0^1 dz \frac{2z-1}{z\bar{z}} \Phi_S^q(z, \zeta_0, \hat{s}), \\ \mathcal{F}_i &= \sum_q \frac{e_q^2}{2} \int_0^1 dz \frac{1}{z\bar{z}} \Phi_i^q(z, \zeta_0, \hat{s}) \quad \text{for } i = A, P, \end{aligned} \quad (12)$$

where we introduce the notation $\bar{z} \equiv 1 - z$. In Eq. (11), $g_T^{\mu\nu}$ and $\epsilon_T^{\mu\nu}$ are transverse tensors,

$$\begin{aligned} g_T^{\alpha\beta} &= g^{\alpha\beta} - n^\alpha \tilde{n}^\beta - n^\beta \tilde{n}^\alpha, \\ \epsilon_T^{\mu\nu} &= \epsilon^{\mu\nu\alpha\beta} \tilde{n}_\alpha n_\beta, \end{aligned}$$

The hadron tensor $T_{\mu\nu}$ written above represents the leading-twist contribution at zeroth order in α_s . When contracted with the polarization vectors of transversely polarized photons, it leads to the leading-twist amplitudes without a helicity flip. However, the longitudinal virtual photon will contribute to the amplitude if one includes the higher-twist corrections [30]. At higher order of α_s , the gluon GDAs also contribute and the transversity gluon GDAs introduce the third transverse tensor [59] $\tau_T^{\mu\nu;\rho\sigma} = (g_T^{\mu\rho} g_T^{\nu\sigma} + g_T^{\mu\sigma} g_T^{\nu\rho} - g_T^{\mu\nu} g_T^{\rho\sigma})/2$, corresponding to amplitudes with a two-unit photon helicity flip.

B. Unpolarized cross section

We sum only over the two polarization states of the antibaryon, and the resulting cross section consists of two components,

$$\frac{d\sigma(S_1)}{d\hat{s}dQ^2 d(\cos\theta) d\varphi} = \frac{1}{2} \frac{d\bar{\sigma}}{d\hat{s}dQ^2 d(\cos\theta) d\varphi} + \frac{d\hat{\sigma}(S_1)}{d\hat{s}dQ^2 d(\cos\theta) d\varphi}. \quad (13)$$

The first term represents the unpolarized cross section, which remains after summing over the polarization states of the baryon. The second term depends on the baryon spin vector S_1 and corresponds to the single-spin correlation.

We introduce a few dimensionless parameters to describe the cross sections for $e^\pm \gamma \rightarrow e^\pm B\bar{B}$,

$$\epsilon = \frac{1-y}{1-y+\frac{y^2}{2}}, \quad y = \frac{q_1 \cdot q_2}{k_1 \cdot q_2}, \quad x = \frac{Q^2}{Q^2+\hat{s}}, \quad \lambda = \frac{1}{(\beta_0)^2}. \quad (14)$$

Given that the cross sections become very cumbersome, particularly when baryon polarizations are included, it is convenient to define some coefficients expressed in terms of ϵ and x ,

$$\begin{aligned} \omega_1 &= 1 - 2x(1-x)(1-\epsilon), & \omega_5 &= \sqrt{\epsilon(1+\epsilon)}\sqrt{2x(1-x)}(2x-1), \\ \omega_2 &= 1 - 2x(1-x)(1+\epsilon), & \omega_6 &= \sqrt{\epsilon(1+\epsilon)}\sqrt{2x(1-x)}, \\ \omega_3 &= 2\epsilon x(1-x), & \omega_7 &= 1 - (1-x)(1-\epsilon), \\ \omega_4 &= 1 - 2x(1-x), & \omega_8 &= 1 - (1-x)(1+\epsilon). \end{aligned} \quad (15)$$

We first calculate the unpolarized cross sections, and the contribution of subprocess (a) to the differential cross section is obtained using the hadron tensor of Eq. (11),

$$\begin{aligned} \frac{d\bar{\sigma}_G}{d\hat{s}dQ^2d(\cos\theta)d\varphi} &= \frac{\alpha_{\text{em}}^3\beta_0}{8\pi s^2 Q^2} \frac{1}{1-\epsilon} \left\{ |\mathcal{F}_A|^2 - |\mathcal{F}_S|^2 + 2\text{Re}(\mathcal{F}_A\mathcal{F}_P^*) + \frac{\hat{s}}{4m^2}(|\mathcal{F}_P|^2 + |\mathcal{F}_S|^2) \right. \\ &\quad \left. + (\beta_0)^2 \cos^2\theta \left[|\mathcal{F}_V|^2 + 2\text{Re}(\mathcal{F}_S\mathcal{F}_V^*) - |\mathcal{F}_A|^2 \right] - (\beta_0)^4 \cos^4\theta |\mathcal{F}_V|^2 \right\}, \end{aligned} \quad (16)$$

where the four twist-2 GDAs appear in the timelike Compton FFs, and this GDA contribution is independent on the azimuthal angle φ . It is straightforward to calculate the contribution of the bremsstrahlung subprocess (b), which are described by the timelike baryon EM FFs of Eq. (8),

$$\begin{aligned} \frac{d\bar{\sigma}_B}{d\hat{s}dQ^2d(\cos\theta)d\varphi} &= \frac{\alpha_{\text{em}}^3\beta_0^3}{4\pi s^2} \frac{1}{\epsilon\hat{s}} \left\{ \omega_1(2\lambda-1)|G_M|^2 + \left[\omega_2|G_M|^2 + 2\omega_3(\lambda-1)(|G_E|^2 - |G_M|^2) \right] \cos^2\theta \right. \\ &\quad \left. + \left[\omega_3|G_M|^2 + \omega_4(\lambda-1)(|G_E|^2 - |G_M|^2) \right] \sin^2\theta + \omega_5 \left[(\lambda-1)|G_E|^2 - \lambda|G_M|^2 \right] \right. \\ &\quad \left. \times \sin(2\theta)\cos\varphi - \omega_3 \left[(\lambda-1)|G_E|^2 - \lambda|G_M|^2 \right] \sin^2\theta \cos(2\varphi) \right\}, \end{aligned} \quad (17)$$

and the dependence on the azimuthal angle appears in this contribution. Then, the interference contribution of the two amplitudes of subprocesses (a) and (b) is written as

$$\begin{aligned} \frac{d\bar{\sigma}_I}{d\hat{s}dQ^2d(\cos\theta)d\varphi} &= e_l \frac{\alpha_{\text{em}}^3\beta_0}{8\pi s^2} \frac{\sqrt{2}\beta_0}{Q\sqrt{\hat{s}\epsilon(1-\epsilon)}} \left\{ 2\omega_6 [\text{Re}(G_M^*\mathcal{F}_V) + \text{Re}(G_E^*\mathcal{F}_S)] \cos\theta - 2(\beta_0)^2\omega_6 [\lambda\text{Re}(G_M^*\mathcal{F}_V) \right. \\ &\quad \left. - (\lambda-1)\text{Re}(G_E^*\mathcal{F}_V)] \cos^3\theta + 2[\omega_7\text{Re}(G_M^*\mathcal{F}_A) + \omega_8\text{Re}(G_E^*\mathcal{F}_S)] \sin\theta \cos\varphi \right. \\ &\quad \left. - (\beta_0)^2\omega_8 [\lambda\text{Re}(G_M^*\mathcal{F}_V) - (\lambda-1)\text{Re}(G_E^*\mathcal{F}_V)] \sin(2\theta) \cos\theta \cos\varphi \right\}, \end{aligned} \quad (18)$$

where e_l is the charge of the lepton e^\pm . After integration over azimuthal angle, the differential cross sections are expressed as

$$\begin{aligned} \frac{d\bar{\sigma}_G}{d\hat{s}dQ^2d(\cos\theta)} &= \frac{\alpha_{\text{em}}^3\beta_0}{4s^2 Q^2} \frac{1}{1-\epsilon} \left\{ |\mathcal{F}_A|^2 - |\mathcal{F}_S|^2 + 2\text{Re}(\mathcal{F}_A\mathcal{F}_P^*) + \frac{\hat{s}}{4m^2}(|\mathcal{F}_P|^2 + |\mathcal{F}_S|^2) \right. \\ &\quad \left. + (\beta_0)^2 \cos^2\theta \left[|\mathcal{F}_V|^2 + 2\text{Re}(\mathcal{F}_S\mathcal{F}_V^*) - |\mathcal{F}_A|^2 \right] - (\beta_0)^4 \cos^4\theta |\mathcal{F}_V|^2 \right\}, \\ \frac{d\bar{\sigma}_B}{d\hat{s}dQ^2d(\cos\theta)} &= \frac{\alpha_{\text{em}}^3\beta_0^3}{2s^2} \frac{1}{\epsilon\hat{s}} \left\{ \omega_1(2\lambda-1)|G_M|^2 + \left[\omega_2|G_M|^2 + 2\omega_3(\lambda-1)(|G_E|^2 - |G_M|^2) \right] \cos^2\theta \right. \\ &\quad \left. + \left[\omega_3|G_M|^2 + \omega_4(\lambda-1)(|G_E|^2 - |G_M|^2) \right] \sin^2\theta \right\}, \\ \frac{d\bar{\sigma}_I}{d\hat{s}dQ^2d(\cos\theta)} &= e_l \frac{\alpha_{\text{em}}^3\beta_0}{4s^2} \frac{\sqrt{2}\beta_0}{Q\sqrt{\hat{s}\epsilon(1-\epsilon)}} \left\{ 2\omega_6 [\text{Re}(G_M^*\mathcal{F}_V) + \text{Re}(G_E^*\mathcal{F}_S)] \cos\theta \right. \\ &\quad \left. - 2(\beta_0)^2\omega_6 [\lambda\text{Re}(G_M^*\mathcal{F}_V) - (\lambda-1)\text{Re}(G_E^*\mathcal{F}_V)] \cos^3\theta \right\}. \end{aligned} \quad (19)$$

In the cross sections, the physical quantities we are interested in are the baryon GDAs, which only exist in Eqs. (16) and (18). If we take the difference of the cross sections in the processes $e^-\gamma \rightarrow e^-B\bar{B}$ and $e^+\gamma \rightarrow e^+B\bar{B}$, only the interference term will remain. Thus, we can employ the lepton charge asymmetry to extract the GDAs from the interference term, in close analogy to the deeply virtual Compton scattering. In addition, one can make use of the exchange of $(\theta, \varphi) \rightarrow (\pi - \theta, \pi + \varphi)$ in the cross sections. The charge conjugation of the baryon–antibaryon pairs differs between subprocesses (a) and (b). Consequently, Eqs. (16) and (17) remain unchanged under this exchange, whereas Eq. (18) changes sign. We can define a asymmetry as

$$\bar{A}(\theta, \varphi) = \frac{\frac{d\bar{\sigma}(\theta, \varphi)}{d\cos\theta d\varphi} - \frac{d\bar{\sigma}(\pi - \theta, \varphi + \pi)}{d\cos\theta d\varphi}}{\frac{d\bar{\sigma}(\theta, \varphi)}{d\cos\theta d\varphi} + \frac{d\bar{\sigma}(\pi - \theta, \varphi + \pi)}{d\cos\theta d\varphi}}, \quad (20)$$

and only the interference contribution survives in the numerator. Furthermore, a forward-backward asymmetry may be defined by integrating the azimuthal angle φ from $\pi/2$ to $3\pi/2$ and subtracting the integral over the complementary region,

$$\bar{A}_{FB}(\theta) = \frac{\int_{\pi/2}^{3\pi/2} d\varphi \frac{d\bar{\sigma}(\theta, \varphi)}{d\cos\theta d\varphi} - \int_{3\pi/2}^{2\pi} d\varphi \frac{d\bar{\sigma}(\pi - \theta, \varphi)}{d\cos\theta d\varphi} - \int_0^{\pi/2} d\varphi \frac{d\bar{\sigma}(\pi - \theta, \varphi)}{d\cos\theta d\varphi}}{\int_{\pi/2}^{3\pi/2} d\varphi \frac{d\bar{\sigma}(\theta, \varphi)}{d\cos\theta d\varphi} + \int_{3\pi/2}^{2\pi} d\varphi \frac{d\bar{\sigma}(\pi - \theta, \varphi)}{d\cos\theta d\varphi} + \int_0^{\pi/2} d\varphi \frac{d\bar{\sigma}(\pi - \theta, \varphi)}{d\cos\theta d\varphi}}. \quad (21)$$

The numerator of \bar{A}_{FB} is denoted as $\int_{\Delta\varphi} d\varphi \frac{d\Delta\bar{\sigma}(\theta, \varphi)}{d\cos\theta d\varphi}$, which is expressed as

$$\begin{aligned} \frac{d\bar{\sigma}_{FB}}{d\hat{s}dQ^2d(\cos\theta)} &= \int_{\Delta\varphi} d\varphi \frac{d\Delta\bar{\sigma}(\theta, \varphi)}{d\cos\theta d\varphi} \\ &= e_I \frac{\alpha_{\text{em}}^3 \beta_0}{2\pi s^2} \frac{\sqrt{2}\beta_0}{Q\sqrt{\hat{s}}(1-\epsilon)} \left\{ \pi\omega_6 [\text{Re}(G_M^* \mathcal{F}_V) + \text{Re}(G_E^* \mathcal{F}_S)] \cos\theta - \pi(\beta_0)^2 \omega_6 [\lambda \text{Re}(G_M^* \mathcal{F}_V) \right. \\ &\quad \left. - (\lambda - 1) \text{Re}(G_E^* \mathcal{F}_V)] \cos^3\theta - 2 [\omega_7 \text{Re}(G_M^* \mathcal{F}_A) + \omega_8 \text{Re}(G_E^* \mathcal{F}_S)] \sin\theta \right. \\ &\quad \left. + (\beta_0)^2 \omega_8 [\lambda \text{Re}(G_M^* \mathcal{F}_V) - (\lambda - 1) \text{Re}(G_E^* \mathcal{F}_V)] \sin(2\theta) \cos\theta \right\}. \end{aligned} \quad (22)$$

This yields a new observable for accessing the baryon GDAs from the interference term.

C. Single-spin correlation

We now present the single-spin correlation for $e^\pm\gamma \rightarrow e^\pm B\bar{B}$. The pure QCD contribution is written as the timelike Compton FFs,

$$\frac{d\hat{\sigma}_G(S_1)}{d\hat{s}dQ^2d(\cos\theta)d\varphi} = \frac{\alpha_{\text{em}}^3 \beta_0^2}{32\pi s^2 Q^2 (1-\epsilon)} \frac{\sqrt{\hat{s}}}{m} [-\beta_0 \sin(2\theta) \text{Im}(\mathcal{F}_V \mathcal{F}_S^*) + 2 \sin\theta \text{Im}(\mathcal{F}_A \mathcal{F}_P^*)] S_1^y. \quad (23)$$

In contrast, its counterpart, Eq. (16), probes the real parts of the products of two Compton FFs $\mathcal{F}_i \mathcal{F}_j^*$, while by including baryon polarizations, we gain access to their imaginary parts. This provides complementary information to the unpolarized cross sections. In addition, we can also sum over the two polarization states of the baryon and obtain the single-spin correlation that is dependent on the spin vector S_2 of the antibaryon using the following replacements,

$$\begin{aligned} (\theta, \varphi) &\rightarrow (\pi - \theta, \pi + \varphi), \\ (S_1^x, S_1^y, S_1^z) &\rightarrow (-S_2^x, -S_2^y, S_2^z). \end{aligned} \quad (24)$$

Then, the second term in Eq. (23) changes sign for the S_2 case, whereas the sign of the first term remains unchanged. Thus, one can infer that the spin vector of the baryon or antibaryon is always perpendicular to the hadron plane, as illustrated in Fig. 1. The first term in Eq. (23) induces a parallel alignment between the spin vectors of the produced baryon and antibaryon, while the second term leads to an antiparallel alignment.

The contribution of the bremsstrahlung subprocess to the differential cross section is expressed as

$$\begin{aligned} \frac{d\hat{\sigma}_B(S_1)}{d\hat{s}dQ^2d(\cos\theta)d\varphi} &= \frac{\alpha_{\text{em}}^3 \beta_0}{4\pi s^2 \epsilon \hat{s}} \frac{m}{\sqrt{\hat{s}}} \text{Im}(G_M G_E^*) \left\{ 2 [\omega_3 \sin\theta \sin(2\varphi) - \omega_5 \cos\theta \sin\varphi] S_1^x \right. \\ &\quad \left. + [\omega_2 \sin(2\theta) + 2\omega_5 \cos(2\theta) \cos\varphi - 2\omega_3 \sin(2\theta) \cos^2\varphi] S_1^y \right\}, \end{aligned} \quad (25)$$

where the coefficients ω_i are defined by Eq. (15). Similarly, we can obtain the single-spin correlation for the S_2 case using the replacements in Eq. (24). The spin vector of the baryon (or antibaryon) lies entirely within the x - y plane of its rest frame. Finally, we calculate the interference contribution of subprocesses (a) and (b),

$$\begin{aligned} \frac{d\hat{\sigma}_I(S_1)}{d\hat{s}dQ^2d(\cos\theta)d\varphi} = & \frac{e_l\alpha_{\text{em}}^3\beta_0}{8\pi s^2Q\sqrt{2\hat{s}\epsilon(1-\epsilon)}} \left\{ \left[\beta_0 \left(\omega_8 \text{Im}(G_M^* \mathcal{F}_S) \sin\varphi + \omega_8 \frac{4m^2}{\hat{s}} \text{Im}(G_M^* \mathcal{F}_V) \cos^2\theta \sin\varphi \right. \right. \right. \\ & + \omega_7 \frac{4m^2}{\hat{s}} \text{Im}(G_E^* \mathcal{F}_A) \sin^2\theta \sin\varphi \Big) + \omega_7 \text{Im}\left(G_M^* \left(\mathcal{F}_P + \frac{4m^2}{\hat{s}} \mathcal{F}_A \right)\right) \cos\theta \sin\varphi \Big] \frac{\sqrt{\hat{s}}}{m} S_1^x \\ & + \left[\beta_0 \left(\omega_6 \text{Im}(G_M^* \mathcal{F}_S) \sin\theta - \omega_8 \text{Im}\left(G_M^* \left(\mathcal{F}_S + \frac{4m^2}{\hat{s}} \mathcal{F}_V \right)\right) \cos\theta \cos\varphi + \omega_6 \frac{2m^2}{\hat{s}} \right. \right. \\ & \times \text{Im}\left((G_M^* - G_E^*) \mathcal{F}_V\right) \sin(2\theta) \cos\theta + \omega_8 \frac{2m^2}{\hat{s}} \text{Im}\left((G_M^* - G_E^*) \mathcal{F}_V\right) \sin(2\theta) \sin\theta \cos\varphi \Big) \\ & - \omega_7 \text{Im}\left(G_M^* \left(\mathcal{F}_P + \frac{4m^2}{\hat{s}} \mathcal{F}_A \right)\right) \cos\varphi \Big] \frac{\sqrt{\hat{s}}}{m} S_1^y + \left[2\omega_7 \text{Im}\left(G_E^* \left(\mathcal{F}_P + \frac{4m^2}{\hat{s}} \mathcal{F}_A \right)\right) \sin\theta \sin\varphi \right. \\ & \left. \left. \left. - \beta_0 \left(\omega_7 \text{Im}(G_M^* \mathcal{F}_A) - \omega_8 \text{Im}(G_M^* \mathcal{F}_V) \right) \sin(2\theta) \sin\varphi \right] S_1^z \right\}. \end{aligned} \quad (26)$$

To obtain the counterpart of Eq. (26) that depends on S_2 , an additional minus sign must be included following the replacements in Eq. (24). The interference term shows that the produced baryon or antibaryon can be polarized along the z -axis of its rest frame, which does not exist in Eqs. (23) and (25).

IV. NUMERICAL ESTIMATES OF THE CROSS SECTIONS

In this section, we present numerical estimates for $e^\pm\gamma \rightarrow e^\pm p\bar{p}$ cross sections and asymmetries, using models of the proton EM FFs based on experimental information and a simple but motivated model for proton GDAs derived in our former work [36]. This will provide guidance for future experimental measurements that will ultimately lead to more realistic models of GDAs.

Much experimental information exists on the modulus of the proton EM FFs on the spacelike and timelike regions [60–74]. As discussed in [36], we neglect the unknown phases of the FFs and use a two component description [68] that fits experimental data in a satisfactory way. In this work, we do not repeat the parameterization of proton EM FFs, as the details can be found in Refs. [36, 68].

Our model [36] for the nucleon-antinucleon GDAs is based on an analogy with the measured $\pi\pi$ GDAs and the decomposition coming from the evolution equations (which are the same for both GDAs). The phases of the $N\bar{N}$ GDAs are unknown and we neglect their effects, while the moduli are constrained by the sum rules which relate them to the quark momentum content of the hadron (the R_q measuring the ratio of momentum carried by quark q in the hadron, as measured in deep inelastic scattering). This allows us to estimate the proton Compton FFs \mathcal{F}_S and \mathcal{F}_V as:

$$\begin{aligned} \mathcal{F}_S &= \sum_q \frac{e_q^2}{2} \int_0^1 dz \frac{2z-1}{z\bar{z}} \Phi_{N\bar{N}}^q(z, \zeta_0, \hat{s}), \\ \zeta_0 \mathcal{F}_V &= \mathcal{F}_S \cos\theta, \end{aligned} \quad (27)$$

with

$$\Phi_{N\bar{N}}^q(z, \cos\theta, \hat{s}) = \frac{3(2\alpha+3)}{5B(\alpha+1, \alpha+1)} z^\alpha (1-z)^\alpha (2z-1) \left[\tilde{B}_{10}^q(\hat{s}) + \tilde{B}_{12}^q(\hat{s}) P_2(\cos\theta) \right], \quad (28)$$

where $\alpha = 1.157$ is obtained from fits to $\pi\pi$ experimental data and is very close to the asymptotic prediction $\alpha = 1$. $B(a, b)$ are Euler's beta functions. In our simple model, we neglect the imaginary phases for the complex functions \tilde{B}_{nl} and write,

$$\begin{aligned} \tilde{B}_{10}^q(\hat{s}) &= -\frac{10R_q}{9} \left(1 + \frac{2m^2}{\hat{s}} \right) F_q(\hat{s}), \\ \tilde{B}_{12}^q(\hat{s}) &= \frac{10R_q}{9} \left(1 - \frac{4m^2}{\hat{s}} \right) F_q(\hat{s}), \end{aligned} \quad (29)$$

where $R_u = 1/3$, $R_d = 1/6$, and m is the proton mass instead of the pion mass. $F_q(\hat{s})$ is the monopole FF,

$$F_q(\hat{s}) = \frac{1}{[1 + (\hat{s} - 4m^2)/\Lambda^2]}, \quad (30)$$

where $\Lambda = 1.928$ GeV is the cut-off parameter. We also neglect resonance contributions in the GDAs, which are expected to play an important role in the resonance regions. The Compton FFs \mathcal{F}_A and \mathcal{F}_P are related to the axial-vector GDAs Φ_A^q and Φ_P^q , respectively. Since no studies on the axial-vector GDAs are currently available, we assume that \mathcal{F}_A and \mathcal{F}_P are proportional to the axial charge,

$$\mathcal{F}_A = \mathcal{F}_P = g_A \mathcal{F}_S, \quad (31)$$

with

$$g_A = e_u g_A^u + e_d g_A^d. \quad (32)$$

In this work, we adopt $g_A^u = 0.832$ and $g_A^d = -0.417$ for the axial charges [75].

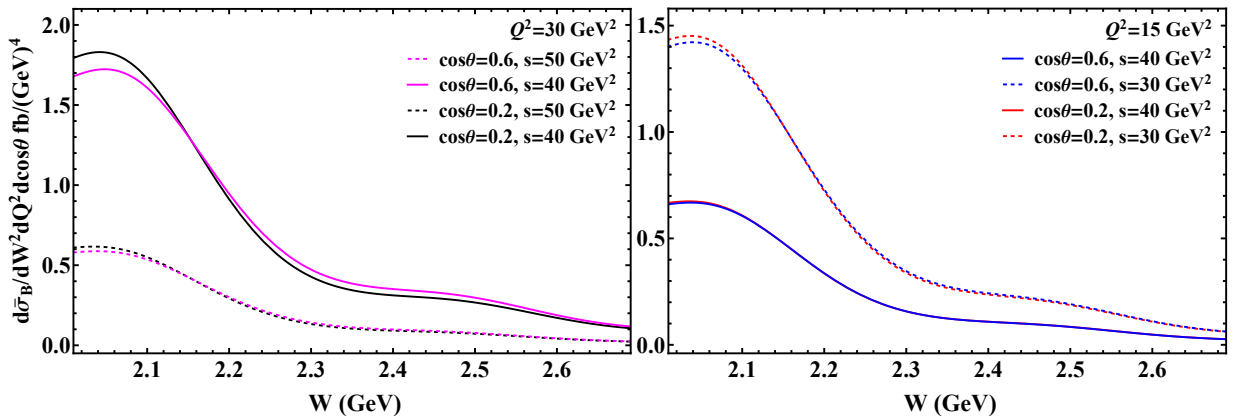


FIG. 4: The differential cross section of the bremsstrahlung process in $e^- \gamma \rightarrow e^- p\bar{p}$.

In our numerical estimates, the kinematics are chosen according to Belle II for $e^- \gamma \rightarrow e^- p\bar{p}$. We use the differential cross sections after integration over azimuthal angle, which are given in Eqs. (19) and (22). In Fig. 4, the cross section of the bremsstrahlung process is shown using the model for the proton EM FFs. In the left panel, we set $Q^2 = 30$ GeV 2 and take $s = 40$ GeV 2 and 50 GeV 2 as typical values, where the black (magenta) curves correspond to $\cos \theta = 0.2$ (0.6). The invariant mass of the proton-antiproton pair is chosen within the range $2.0 \text{ GeV} < W = \sqrt{\hat{s}} < 2.7 \text{ GeV}$. The bremsstrahlung cross section shows a weak dependence on the polar angle $\cos \theta$. In the right panel of Fig. 4, we reduce Q^2 from 30 GeV 2 to 15 GeV 2 , where $s = 30$ GeV 2 and 40 GeV 2 are used, and the red (blue) curves correspond to $\cos \theta = 0.2$ (0.6). The bremsstrahlung contribution varies significantly when comparing the results at $Q^2 = 15$ GeV 2 and $Q^2 = 30$ GeV 2 in Fig. 4 for fixed $s = 40$ GeV 2 . This variation originates from the parameter ϵ . For instance, we have $\epsilon = 0.81$ at $W = 2.1$ GeV, $Q^2 = 15$ GeV 2 , and $s = 40$ GeV 2 , while increasing Q^2 to 30 GeV 2 reduces ϵ to 0.27. Consequently, according to Eq. (19), the corresponding cross section becomes about three times larger, in agreement with the behavior observed in Fig. 4. Note that our predictions of the bremsstrahlung contribution can be considered as accurate estimates, since only the modulus of the timelike proton electric and magnetic FFs are used as inputs, which have been well constrained by experiment.

The differential cross section of the pure QCD process is depicted in Fig. 5, where the model of proton-antiproton GDAs is used. The same conventions are adopted as Fig. 4, and we choose $Q^2 = 30$ GeV 2 and 15 GeV 2 in the right and left panels, respectively. Compared with the bremsstrahlung contribution shown in Fig. 4, the GDA contribution to the process $e^- \gamma \rightarrow e^- p\bar{p}$ is smaller at $Q^2 = 30$ GeV 2 . However, the GDA contribution increases significantly when Q^2 decreases from 30 GeV 2 to 15 GeV 2 . This enhancement arises from the prefactor $1/[Q^2(1 - \epsilon)]$ in Eq. (19). As Q^2 changes from 30 GeV 2 to 15 GeV 2 with fixed $W = 2.1$ GeV and $s = 40$ GeV 2 , this factor increases by approximately an order of magnitude, which is consistent with our numerical results for the GDA contribution. Thus, we can find a kinematical region where the GDA contribution may be larger than the bremsstrahlung contribution, which should be helpful for the extraction of the baryon GDAs.

For the interference term of two subprocesses, we use Eq. (22) instead of Eq. (19) for numerical estimates since more GDAs can be extracted from the angular dependence in this forward-backward asymmetry. The differential cross

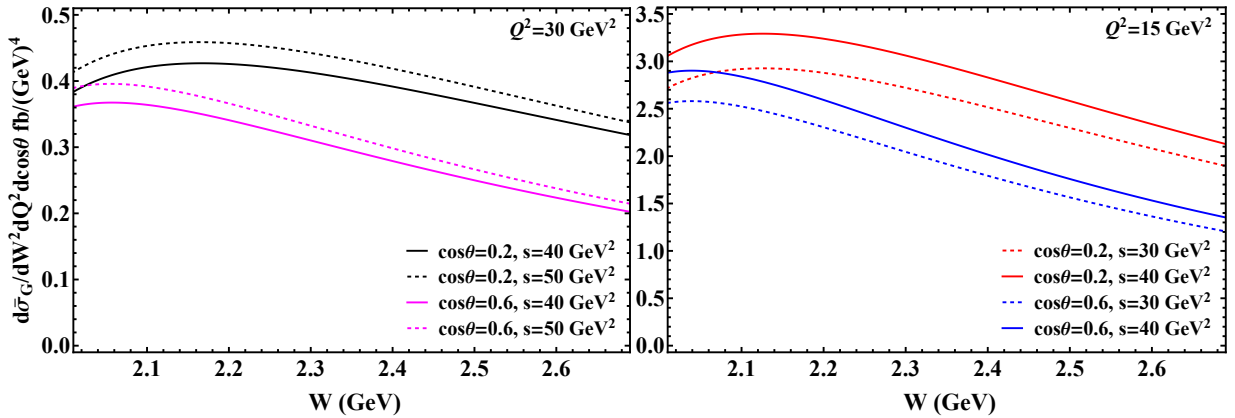


FIG. 5: The differential cross section of the pure QCD contribution in $e^- \gamma \rightarrow e^- p\bar{p}$.

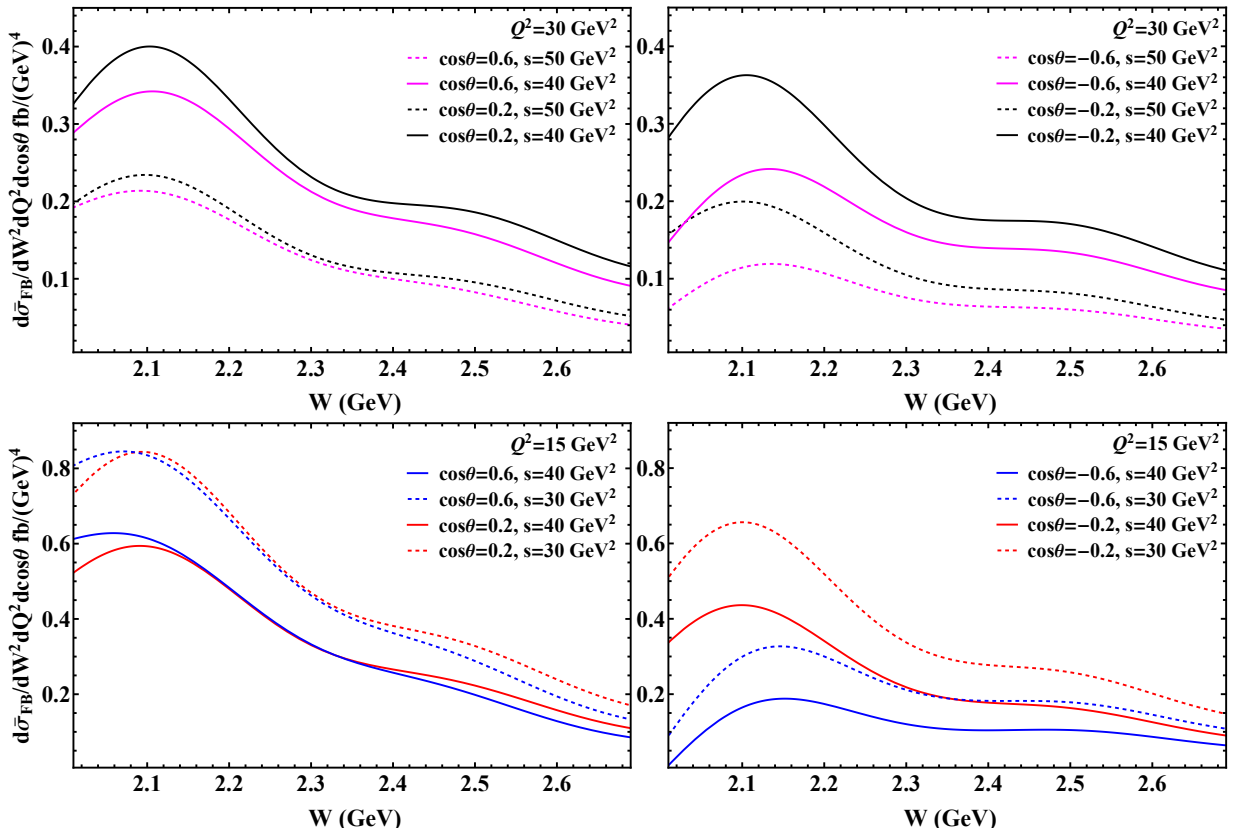


FIG. 6: The cross section difference (Eq.22) allows to measure the interference term of $e^- \gamma \rightarrow e^- p\bar{p}$. It depends on the invariant mass of the proton-antiproton pair and on the polar angle θ of the nucleon.

section of Eq. (22) is depicted in Fig. 6. In the top panel, we take $\cos \theta = \pm 0.2$ (± 0.6) for the black (magenta) curves, with $Q^2 = 30 \text{ GeV}^2$ fixed. The solid and dashed lines correspond to $s = 40 \text{ GeV}^2$ and $s = 50 \text{ GeV}^2$, respectively. The magnitude of the interference term is comparable to that of the pure QCD contribution at $Q^2 = 30 \text{ GeV}^2$, as shown in Fig. 5. In the bottom panel, $s = 30 \text{ GeV}^2$ (40 GeV^2) is fixed for the dashed (solid) curves at $Q^2 = 15 \text{ GeV}^2$, with the red and blue curves corresponding to $\cos \theta = \pm 0.2$ and $\cos \theta = \pm 0.6$, respectively. An enhancement of the interference term is observed when Q^2 decreases from 30 GeV^2 to 15 GeV^2 , which also arises from the prefactor in Eq. (22). Our numerical results can only be regarded as order-of-magnitude estimates for the interference term and the pure QCD contribution, since the proton-antiproton GDAs are poorly known. Further theoretical studies of GDAs are necessary to obtain precise predictions, and precise experimental analysis of the reaction is mostly needed.

After integrating over the azimuthal angle, one can see that the dependence on S_1^x and S_1^z disappears in the single-

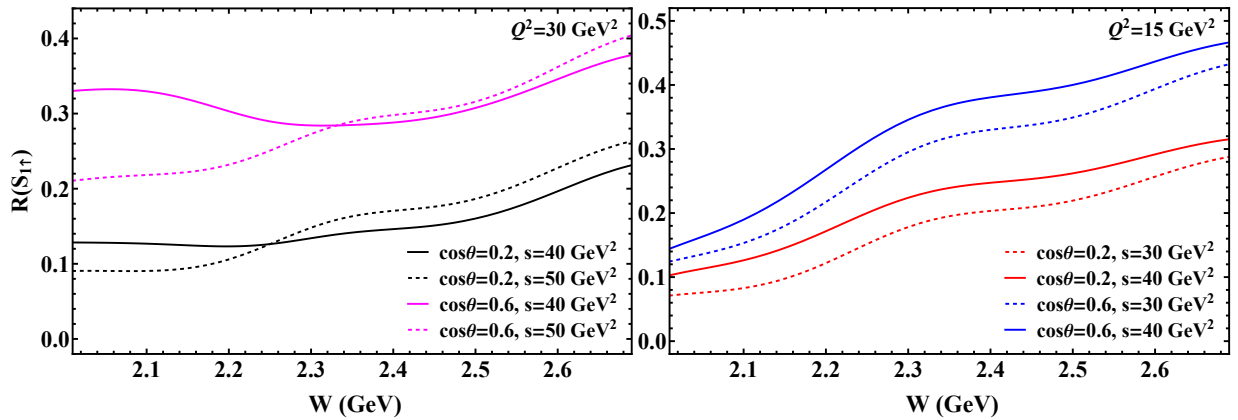


FIG. 7: The estimate of ratio $R(S_{1\uparrow})$ in $e^-\gamma \rightarrow e^- p\bar{p}$ using models of the proton EM FFs and Compton FFs.

spin correlation. Thus, the y-axis is chosen as the polarization direction in the rest frame of the baryon. We can express the spin vector of the spin-up baryon as

$$S_{1\uparrow}^\mu = (0, 0, 1, 0), \quad (33)$$

and $S_{1\downarrow}^\mu = -S_{1\uparrow}^\mu$ for the spin-down state. The cross sections for the production of spin-up and spin-down baryons are given respectively by

$$\begin{aligned} d\sigma(S_{1\uparrow}) &= \frac{1}{2} d\bar{\sigma} + d\hat{\sigma}(S_{1\uparrow}), \\ d\sigma(S_{1\downarrow}) &= \frac{1}{2} d\bar{\sigma} - d\hat{\sigma}(S_{1\uparrow}). \end{aligned} \quad (34)$$

To see the polarization effect, one can define the following ratio using the cross sections derived in Sec. III,

$$R(S_{1\uparrow}) = \left[\frac{d\hat{\sigma}(S_{1\uparrow})}{d\hat{s}dQ^2d(\cos\theta)} \right] / \left[\frac{1}{2} \frac{d\bar{\sigma}}{d\hat{s}dQ^2d(\cos\theta)} \right]. \quad (35)$$

The single-spin correlation $d\hat{\sigma}$ is proportional to the terms $\text{Im}(F_i F_j^*)$, where F_i represents a EM FF or Compton FF as indicated by Eqs. (23), (25), and (26). However, the phases of these FFs, $F_i = |F_i|e^{i\delta_i}$, are still unknown, and there is no reason to assume they vanish. In this work, we show the maximal single-spin correlation by setting all $\sin(\delta_i - \delta_j) = 1$ in $\text{Im}(F_i F_j^*)$. The numerical estimate of the ratio $R(S_{1\uparrow})$ is shown in Fig. 7, based on models of the proton EM FFs and Compton FFs. We choose typical values for s and Q^2 according to the kinematics of Belle II. The colors of curves indicate the different $\cos\theta$, with the same conventions as Fig. 4. We can infer that the polarization effect is sizable in the cross section.

V. SUMMARY

Hadronic GPDs and GDAs are three-dimensional functions that characterize the internal structure of hadrons. The second moments of GPDs and GDAs give rise to the GFFs of hadrons in the spacelike and timelike regions, respectively, which reveal key information about hadron structure. As most hadrons are not stable, it is difficult to access their GPDs using exclusive processes. However, hadronic GDAs probed through hadron-pair production processes such as $\gamma^*\gamma \rightarrow B\bar{B}$ and $\gamma^*\gamma \rightarrow B\bar{B}\gamma$ provide access not only to nucleons but also to unstable baryons such as Λ and Σ .

Recently, the Belle Collaboration reported the cross section for $\gamma^*\gamma \rightarrow \pi^0\pi^0$, where the photons are emitted from the e^\pm beams [38]. The pion GFFs were subsequently extracted from these experimental data for the first time [29]. In this work, we extend the GDA study to a spin-1/2 baryon-antibaryon pair, namely $e^\pm\gamma \rightarrow e^\pm B\bar{B}$, which can be measured at Belle II, the proposed STCF, and electron-ion colliders. In this process, the baryon GDAs are involved in the two-photon fusion subprocess with the C -even baryon-antibaryon pairs. In addition, there is the bremsstrahlung subprocess, and the C -odd baryon-antibaryon pairs are produced. We calculate the theoretical cross sections for $e^\pm\gamma \rightarrow e^\pm B\bar{B}$. The interference contribution of two subprocesses can be extracted using the lepton

charge asymmetry, which are expressed in terms of the baryon GDAs and EM FFs. Since one can determine the spin vectors of baryons from their decays such as $\Lambda \rightarrow N\pi$ and $\Sigma \rightarrow N\pi$, we also include the spin vector of the baryon (or antibaryon), and define the single-spin correlation, from which additional information on the baryon GDAs can be probed. We use motivated models of EM FFs and GDAs to present the numerical estimates for the process $e^-\gamma \rightarrow e^-p\bar{p}$, where the kinematics are chosen according to the Belle II experiment. Our results show that we can find a kinematical region where the GDA contribution may dominate the cross section, which can be used for the experimental measurements of this process. Our study thus provides useful guidance for the future extraction of baryon GDAs at Belle II.

Acknowledgments

Qin-Tao Song was supported by the National Natural Science Foundation of China under Grant Number 12005191.

-
- [1] D. Müller, D. Robaschik, B. Geyer, F. M. Dittes, and J. Hořejši, *Fortsch. Phys.* **42**, 101 (1994), hep-ph/9812448.
- [2] M. Diehl, T. Gousset, B. Pire, and O. Teryaev, *Phys. Rev. Lett.* **81**, 1782 (1998), hep-ph/9805380.
- [3] M. V. Polyakov, *Nucl. Phys. B* **555**, 231 (1999), hep-ph/9809483.
- [4] X.-D. Ji, *Phys. Rev. Lett.* **78**, 610 (1997), hep-ph/9603249.
- [5] A. V. Radyushkin, *Phys. Lett. B* **449**, 81 (1999), hep-ph/9810466.
- [6] M. Burkardt, *Phys. Rev. D* **62**, 071503 (2000), [Erratum: *Phys. Rev. D* 66, 119903 (2002)], hep-ph/0005108.
- [7] J. P. Ralston and B. Pire, *Phys. Rev. D* **66**, 111501 (2002), hep-ph/0110075.
- [8] M. Diehl, *Eur. Phys. J. C* **25**, 223 (2002), [Erratum: *Eur. Phys. J. C* 31, 277–278 (2003)], hep-ph/0205208.
- [9] B. Pire and L. Szymanowski, *Phys. Lett. B* **556**, 129 (2003), hep-ph/0212296.
- [10] E. Leader and C. Lorcé, *Phys. Rept.* **541**, 163 (2014), 1309.4235.
- [11] X. Ji, F. Yuan, and Y. Zhao, *Nature Rev. Phys.* **3**, 27 (2021), 2009.01291.
- [12] C. A. Aidala, S. D. Bass, D. Hasch, and G. K. Mallot, *Rev. Mod. Phys.* **85**, 655 (2013), 1209.2803.
- [13] M. V. Polyakov, *Phys. Lett. B* **555**, 57 (2003), hep-ph/0210165.
- [14] M. V. Polyakov and P. Schweitzer, *Int. J. Mod. Phys. A* **33**, 1830025 (2018), 1805.06596.
- [15] V. D. Burkert, L. Elouadrhiri, and F. X. Girod, *Nature* **557**, 396 (2018).
- [16] C. Lorcé, H. Moutarde, and A. P. Trawiński, *Eur. Phys. J. C* **79**, 89 (2019), 1810.09837.
- [17] K. Kumerički, *Nature* **570**, E1 (2019).
- [18] V. D. Burkert, L. Elouadrhiri, F. X. Girod, C. Lorcé, P. Schweitzer, and P. E. Shanahan, *Rev. Mod. Phys.* **95**, 041002 (2023), 2303.08347.
- [19] A. Freese and G. A. Miller, *Phys. Rev. D* **104**, 014024 (2021), 2104.03213.
- [20] D. Fujii and M. Tanaka, *Phys. Lett. B* **870**, 139872 (2025).
- [21] H. Dutrieux, T. Meisgny, C. Mezrag, and H. Moutarde, *Eur. Phys. J. C* **85**, 105 (2025), 2410.13518.
- [22] A. García Martín-Caro, M. Huidobro, and Y. Hatta, *Phys. Rev. D* **110**, 034002 (2024), 2312.12984.
- [23] Y. Li and J. P. Vary, *Phys. Rev. D* **109**, L051501 (2024), 2312.02543.
- [24] C. Lorcé and Q.-T. Song, *Phys. Lett. B* **864**, 139433 (2025), 2501.05092.
- [25] T. Hu, X. Cao, S. Xu, Y. Li, X. Zhao, and J. P. Vary, *Phys. Rev. D* **111**, 074031 (2025), 2408.09689.
- [26] W. Broniowski and E. Ruiz Arriola, *Phys. Rev. D* **112**, 054028 (2025), 2503.09297.
- [27] M. Diehl, T. Gousset, and B. Pire, *Phys. Rev. D* **62**, 073014 (2000), hep-ph/0003233.
- [28] N. Kivel, L. Mankiewicz, and M. V. Polyakov, *Phys. Lett. B* **467**, 263 (1999), hep-ph/9908334.
- [29] S. Kumano, Q.-T. Song, and O. V. Teryaev, *Phys. Rev. D* **97**, 014020 (2018), 1711.08088.
- [30] C. Lorcé, B. Pire, and Q.-T. Song, *Phys. Rev. D* **106**, 094030 (2022), 2209.11140.
- [31] C. Lorcé, B. Pire, and Q.-T. Song, in *29th International Workshop on Deep-Inelastic Scattering and Related Subjects* (2022), 2208.12532.
- [32] Q.-T. Song, O. V. Teryaev, and S. Yoshida, *Phys. Lett. B* **868**, 139797 (2025), 2503.11316.
- [33] Z. Lu and I. Schmidt, *Phys. Rev. D* **73**, 094021 (2006), [Erratum: *Phys. Rev. D* 75, 099902 (2007)], hep-ph/0603151.
- [34] B. Pire and Q.-T. Song, *Phys. Rev. D* **107**, 114014 (2023), 2304.06389.
- [35] B. Pire and Q.-T. Song, *Phys. Rev. D* **109**, 074016 (2024), 2311.06005.
- [36] J. Han, B. Pire, and Q.-T. Song, *Phys. Rev. D* **112**, 014048 (2025), 2506.09854.
- [37] S. Bhattacharya, R. Boussarie, B. Pire, and L. Szymanowski (2025), 2507.23529.
- [38] M. Masuda et al. (Belle), *Phys. Rev. D* **93**, 032003 (2016), 1508.06757.
- [39] M. Achasov et al., *Front. Phys. (Beijing)* **19**, 14701 (2024), 2303.15790.
- [40] R. R. Akhmetshin et al. (CMD-3), *Phys. Lett. B* **794**, 64 (2019), 1808.00145.
- [41] M. Ablikim et al. (BESIII), *Nature Phys.* **17**, 1200 (2021), 2103.12486.
- [42] J. P. Lees et al. (BaBar), *Phys. Rev. D* **87**, 092005 (2013), 1302.0055.
- [43] M. Ablikim et al. (BESIII), *Phys. Lett. B* **817**, 136328 (2021), 2102.10337.

- [44] M. Ablikim et al. (BESIII), Phys. Rev. Lett. **124**, 042001 (2020), 1905.09001.
- [45] M. Ablikim et al. (BESIII), Phys. Rev. Lett. **130**, 151905 (2023), 2212.07071.
- [46] M. Ablikim et al. (BESIII), Phys. Rev. D **99**, 092002 (2019), 1902.00665.
- [47] M. Ablikim et al. (BESIII), Phys. Rev. D **97**, 032013 (2018), 1709.10236.
- [48] M. Ablikim et al. (BESIII), Phys. Rev. Lett. **123**, 122003 (2019), 1903.09421.
- [49] M. Ablikim et al. (BESIII), Phys. Rev. D **107**, 072005 (2023), 2303.07629.
- [50] M. Ablikim et al. (BESIII), Phys. Lett. B **814**, 136110 (2021), 2009.01404.
- [51] M. Ablikim et al. (BESIII), Phys. Rev. Lett. **132**, 081904 (2024), 2307.15894.
- [52] M. Ablikim et al. (BESIII), Phys. Rev. D **109**, 034029 (2024), 2312.12719.
- [53] G. Gong et al. (Belle), Phys. Rev. D **107**, 072008 (2023), 2210.16761.
- [54] M. Ablikim et al. (BESIII), Phys. Lett. B **831**, 137187 (2022), 2110.04510.
- [55] M. Ablikim et al. (BESIII), Phys. Lett. B **820**, 136557 (2021), 2105.14657.
- [56] M. Ablikim et al. (BESIII), Phys. Rev. D **103**, 012005 (2021), 2010.08320.
- [57] B. Guo, J. Han, Y.-P. Xie, and X. Chen, Eur. Phys. J. C **85**, 506 (2025), 2501.01267.
- [58] M. Diehl, P. Kroll, and C. Vogt, Eur. Phys. J. C **26**, 567 (2003), hep-ph/0206288.
- [59] A. V. Belitsky and D. Mueller, Phys. Lett. B **486**, 369 (2000), hep-ph/0005028.
- [60] T. Liu and B.-Q. Ma, Phys. Rev. D **92**, 096003 (2015), 1510.07783.
- [61] A. Afanasev, P. G. Blunden, D. Hasell, and B. A. Raue, Prog. Part. Nucl. Phys. **95**, 245 (2017), 1703.03874.
- [62] V. V. Bytev and E. Tomasi-Gustafsson, Phys. Rev. C **99**, 025205 (2019), [Erratum: Phys. Rev. C **106**, 029902 (2022)], 1901.09379.
- [63] Y.-H. Lin, H.-W. Hammer, and U.-G. Meißner, Phys. Rev. Lett. **128**, 052002 (2022), 2109.12961.
- [64] C. McRae and P. G. Blunden, Phys. Rev. C **109**, 015503 (2024), 2309.03892.
- [65] M. V. Galynskii, V. V. Bytev, and V. M. Galynsky, Phys. Rev. D **110**, 096017 (2024), 2408.09249.
- [66] K. S. Kuzmin, N. M. Levashko, and M. I. Krivoruchenko, Phys. Rev. D **111**, 013004 (2025), 2412.13150.
- [67] A. Bianconi and E. Tomasi-Gustafsson, Phys. Rev. Lett. **114**, 232301 (2015), 1503.02140.
- [68] E. Tomasi-Gustafsson, A. Bianconi, and S. Pacetti, Phys. Rev. C **103**, 035203 (2021), 2012.14656.
- [69] E. L. Lomon and S. Pacetti, Phys. Rev. D **85**, 113004 (2012), [Erratum: Phys. Rev. D **86**, 039901 (2012)], 1201.6126.
- [70] R.-Q. Qian, Z.-W. Liu, X. Cao, and X. Liu, Phys. Rev. D **107**, L091502 (2023), 2211.11555.
- [71] B. Yan, C. Chen, X. Li, and J.-J. Xie, Phys. Rev. D **109**, 036033 (2024), 2312.04866.
- [72] G. Huang and R. B. Ferroli (BESIII), Natl. Sci. Rev. **8**, nwab187 (2021), 2111.08425.
- [73] Q.-H. Yang, D. Guo, M.-Y. Li, L.-Y. Dai, J. Haidenbauer, and U.-G. Meißner, JHEP **08**, 208 (2024), 2404.12448.
- [74] X. Cao, J.-P. Dai, and H. Lenske, Phys. Rev. D **105**, L071503 (2022), 2109.15132.
- [75] C. Alexandrou, S. Bacchio, J. Finkenrath, C. Iona, G. Koutsou, Y. Li, and G. Spanoudes, Phys. Rev. D **111**, 054505 (2025), 2412.01535.